Biotribology 35-36 (2023) 100261

Contents lists available at ScienceDirect

Biotribology

journal homepage: www.elsevier.com/locate/biotri

Friction and Contact Temperatures in the Cleaving of Bone and Wood Using Stone Tools – A Case Study in Palaeolithic Tribology

M.A. Masen [a,*], G.C.L. Vlamings [b], D.J. Schipper [c]

[a] Tribology Group, Imperial College London, Exhibition Road, London SW7 2AZ, UK
[b] Eemnes, the Netherlands
[c] Laboratory for Surface Technology and Tribology, University of Twente, Enschede, the Netherlands

ARTICLE INFO

Keywords:
Tribology of wood
Bone and stone materials
Frictional heating
Friction induced phase transformation

ABSTRACT

During archaeological fieldwork wedge-shaped quartz stones that show clearly visible "glossy patches" composed of high quartz have been found. It is generally accepted that these tools have been used to cleave or punch wood and bone materials. For the transformation from quartz to high-quartz to occur, the temperature should exceed 574 °C. The hypothesis tested in this manuscript is that the phase change in the stone tool results from frictional heating during the cleaving action. Dry sliding friction measurements were carried out on a reciprocating tribometer using four types of stone, representing the punch tool, and pine, oak and bovine bone, representing the work piece. Measured coefficients of friction were approximately 0.1 on oak, 0.2 on pine and up to 0.35 on bovine bone, with some minor fluctuations for the different types of stone. These coefficients of friction were inserted into a computational model describing the flash temperatures in a moving contact, from which it was shown that the hypothesis might hold in the case of lydite-bone contact. This means that the glossy patches on the stone tools may have been caused by frictional heating during the cleaving of bone.

1. Introduction

Tribological investigations are increasingly being employed in the field of archaeology, on topics ranging from the surface features of bronze objects [1] to the biomechanical and evolutionary aspects of dinosaur tooth wear [2]. The present work aims to also contribute to this field, by offering a potential, friction-based, explanation for phase transformations observed on stone tools that were used for cleaving operations on wood and bone.

During archaeological fieldwork in the region Het Gooi, 30 km southeast of Amsterdam in The Netherlands, a large number of wedge-shaped stones have been found. A generally accepted hypothesis is that these stones were used as wedges or punches, e.g. for cleaving wood, slaughtering hunt and opening bones to obtain the nutritious marrow from the core of the bone [3–5]. The cleaving action was performed by pressing the so-called working point of a wedge shaped stone against the bone or into the softer wood, followed by repeated impact by a heavier "*hammering*" stone, until the work piece was wedged open, as illustrated in Fig. 1.

Stones that may have been used as wedges or punches come in a wide variety of shapes and sizes, with the longitudinal axis ranging from about 10 mm to over 500 mm and with a wedge angle α between 5° and 50°, depending on their cultural origin. Fig. 2(a) depicts some examples of these stones, which are composed of silicon dioxide (SiO_2), of the mineral varieties flint, milk quartz, quartzite and lydite.

A striking phenomenon that can be observed on many of these wedge-shaped stones are glossy patches located at the geometrical summits on the flanks of the tools; in Fig. 2(b) the typical location of these glossy patches on a stone are illustrated, whilst Fig. 2(c) shows a photograph of the glossy patches on a stone. Previous research [3] has indicated that these glossy patches contain high-quartz, a phase of silicon dioxide that under atmospheric pressure only forms at temperatures above 574 °C [6]. These glossy patches are not observed anywhere else on the stones, such as the tip, which usually has been worked or sharpened using other (stone) tools, nor are they found on the flat face opposing the working point, onto which the hammering stone impacted repeatedly. This appears to rule out the possibility of the glossy tracks being the result of stone-stone interaction.

This work aims to offer a contribution towards explaining the origins of these glossy tracks on the stone tools. The working hypothesis is that the glossy tracks are generated during the normal day-to-day use of the tools: During the cleaving operation, the conditions in the contact cause

* Corresponding author.
E-mail address: m.masen@imperial.ac.uk (M.A. Masen).

https://doi.org/10.1016/j.biotri.2023.100261
Received 1 August 2023; Received in revised form 26 September 2023; Accepted 2 October 2023
Available online 7 October 2023

flash-temperatures surpassing 574 °C, resulting in a phase transformation in the mineral to high-quartz. The investigation presented in this article aims to investigate whether this hypothesis is viable.

2. Temperature Calculations

2.1. Model

Models for the temperature rise in a contact as the result of the sliding interaction between two materials have been described extensively in literature, based on the work of Blok [7], Jaeger [8] and Archard [9]. The temperature rise depends on the amount of energy generated during sliding and the rate at which this energy can be removed from the interface. The generated heat per unit area q during the sliding interaction between two surfaces is given by:

$$q = \frac{\mu \cdot F_N \cdot v^-}{A} \tag{1}$$

With μ the coefficient of friction, F_N the contact load, v^- the velocity difference between the two surfaces and A the area of contact.

The heat generated in the contact will flow into the two bodies. According to Blok's theory [7] the heat flow into the two bodies is divided, or partitioned, such that the maximum temperature obtained inside the two bodies is the same. More recently, using advanced computational models [10], it has been shown that this might lead to an underestimation of the local temperature field and that improved results can be obtained when not just the maximum temperature but the complete temperature fields at the interacting surfaces are taken equal. However, this improved accuracy comes at the cost of increased computational effort.

Solving the temperature problem, Moes [12] describes an equation for the temperature in a sliding contact with contact radius a:

$$\boldsymbol{T} = \boldsymbol{T}_{env} + \boldsymbol{T}_{flash} = \boldsymbol{T}_{env} + \frac{\boldsymbol{\mu} \cdot \boldsymbol{p} \cdot \boldsymbol{\pi} \cdot \boldsymbol{a} \cdot \boldsymbol{v}^-}{\boldsymbol{K}} \tag{2}$$

in which $T_{env}$is the temperature of the surrounding environment, T_{flash} T_{flash} is the flash temperature, p is the contact pressure, v^- the velocity difference between the two contacting surfaces and K the thermal conductivity, which depends on the thermal properties of both bodies in contact and on the operating conditions.

Assuming the heat source q to have a parabolic profile with its minimum values on the leading and trailing edges and a maximum value in the centre, Bosman [11] describes the temperature rise Θ in an elliptic contact with semi-axes a and b:

$$\Theta(x', y, z, t) = \int_0^t \int_{-b}^{b} \int_{-a}^{a} \frac{q \cdot \rho \cdot C_p}{8 \cdot (\tau \cdot \pi \cdot \kappa)^{3/2}} \cdot exp\left(-\frac{(x' - x'' + v \cdot t)^2 + (y - y')^2 + z^2}{4 \cdot \kappa \cdot \tau}\right) dx' \, dy \, d\tau \tag{3}$$

with

$$\boldsymbol{q}(\boldsymbol{x}, \boldsymbol{y}) = \frac{\boldsymbol{3} \cdot \boldsymbol{\mu} \cdot \boldsymbol{v}^- \cdot \boldsymbol{F}_N}{\boldsymbol{2} \cdot \boldsymbol{\pi} \cdot \boldsymbol{a} \cdot \boldsymbol{b}} \cdot \sqrt{\boldsymbol{1} - \left(\frac{\boldsymbol{x}}{\boldsymbol{a}}\right)^2 - \left(\frac{\boldsymbol{y}}{\boldsymbol{b}}\right)^2} \tag{4}$$

This means that the temperature in the contact can be calculated as a function of the contact parameters and the material properties.

2.2. Input Parameters for the Model: Conditions during Use

The input parameters for the thermal model are the material properties of the used tool and the worked counter materials, as well as the conditions during the cleaving process. Whilst material properties of these natural materials may vary, Table 1 lists values obtained from

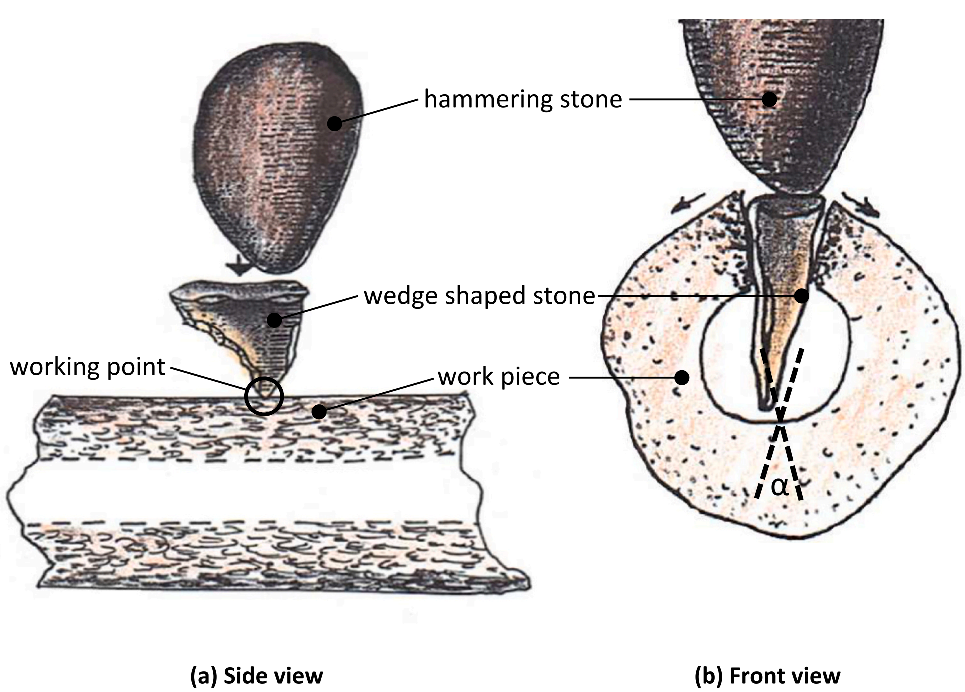

Fig. 1. Illustration of the cleaving process using a stone wedge and a hammering stone, after Vlamings [3].

literature [13,14]. The conditions during use must be estimated.

As previously indicated, the driving force behind the temperature rise in the contact is the energy input, which must be quantified. The users of the tools, respectively *Homo heidelbergensis*, *Homo neanderthalensis* or *Homo sapiens sapiens,* show a considerable variety in corporal dimensions and strength [15,16], but a hammering impact velocity of 5 m·s^{-1} appears an appropriate estimate. The glossy area, marked with S' in Fig. 2, varies in size for the different stones, with typical sizes ranging between 0.5 and 2 cm^2. Depending on the cultural origin, the punch stones can have a top angle α between 5° and 50°, with 22° to 32° being the most common. The last parameter to be determined for the temperature model is the coefficient of friction between the stone tools and the counter material.

3. Friction Measurements

3.1. Experimental Procedure

Reciprocating friction experiments were performed employing the set-up shown in Fig. 3(a). For the tests with a stationary bottom sample of pine and oak the top sample is a stone sample of either flint, quartzite, milky quartz or lydite. For tests with bovine bone only lydite was used due to a limited number of available bone specimens. The applied materials have an anisotropic structure and therefore wood samples with a range of grain directions and bone samples with various cell orientations were included in the experimental programme. Mechanical testing of natural materials is inherently restricted by the available source material, and in this case for the bone specimens the maximum specimen dimension possible was 58 × 18 × 5 mm. This dimension was also adopted for the wood specimens.

During testing, the top sample follows a sinusoidal motion with a maximum velocity of 24 mm·s^{-1}. The bottom sample holder is suspended using parallel positioned weak elastic hinges, giving it a single degree of freedom in translational direction, i.e. the sample holder can only displace horizontally. The horizontal force (i.e. the friction force) is measured using a piezoelectric force transducer. The amplitude of

Table 1
Thermal properties for the materials used in this work [13,14].

	Pine	Oak	Bone	quartz
Thermal Conductivity k [W·m^{-1}·K^{-1}]	0.12	0.16	0.45	3.0
Density ρ [kg·m^{-3}]	400	740	1800	2650
Heat Capacity c [J·kg^{-1}·K^{-1}]	2500	2000	440	70

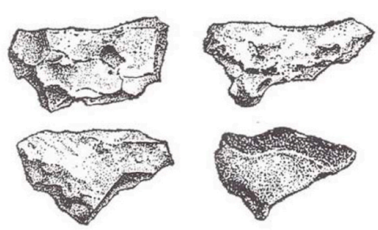

(a)

Some examples of wedge shaped stone tools found during archaeological fieldwork.

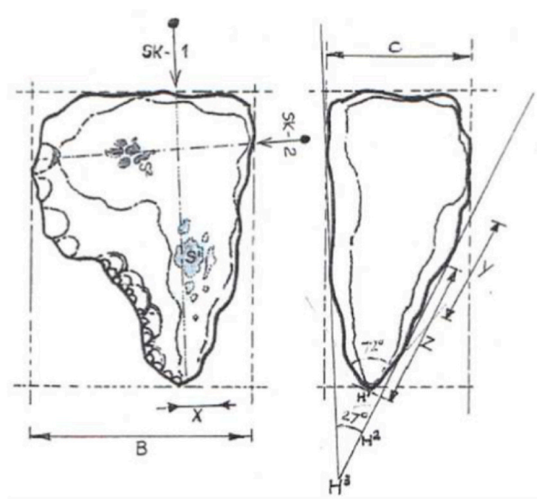

(b)

Typical location of the glossy tracks on the wedge shaped tools, indicated by *S'*.

(c) Photograph showing a glossy patch on the face of one of the stone tools

Fig. 2. Wedge shaped stone tools, after Vlamings [3].

motion of the top-sample is 24 mm, meaning that one period of motion equals a displacement of 96 mm. The normal load is applied using a bellows and the coefficient of friction is calculated from the ratio of the measured value for the friction force and the applied normal load. The applied contact configuration is flat-on-flat, as illustrated in Fig. 3(b).

It needs to be noted that the selected experimental sliding velocity of 24 mm s^{-1} is substantially lower than what would occur during an actual cleaving operation; the possible experimental velocity was limited because of the rather small dimensions of the specimens, but it should be kept in mind that under dry contact conditions the coefficient of friction is rather insensitive to the sliding speed. Furthermore, the friction experiments are performed at ambient environmental conditions and not at elevated temperatures. This means that any effect of thermal degradation of the specimens on their friction behaviour is ignored. However, testing at ambient conditions is thought to more closely resemble the actual cleaving operation, where the contact of the stone tool was typically against a ‘fresh’, thermally non-degraded, surface.

A summary of the conditions of the friction experiment are listed in Table 2.

A typical friction measurement result is shown in Fig. 3(c), in this case for milky quartz sliding against oak. The graph shows the friction measured during two and a half reciprocations. The coefficient of friction shows a repeatable trend within each motion and is constant between reciprocations. From the measured friction graph as shown in Fig. 3, an average value for the coefficient of friction is calculated by including only the data points corresponding to the centre 50% of each reciprocation, (i.e. deleting the first and final 25% of the track) and calculating the average absolute deviation of the remaining data points. In this way, data representing in the reciprocation points (i.e. where the velocity is zero) are ignored and effects that are the result of any (minor) misalignment are corrected.

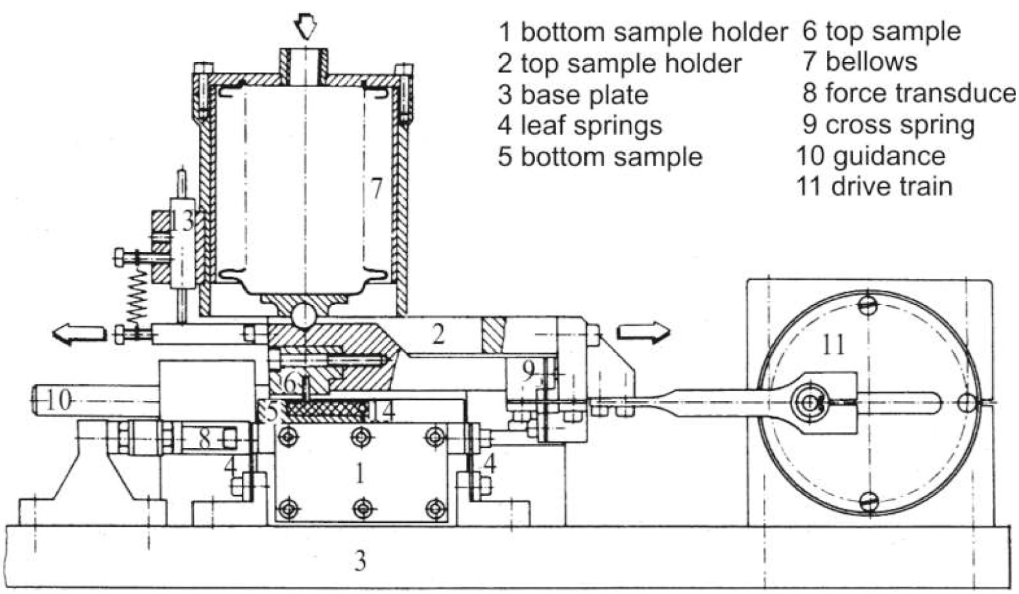

(a) Schematic of the reciprocating tribometer

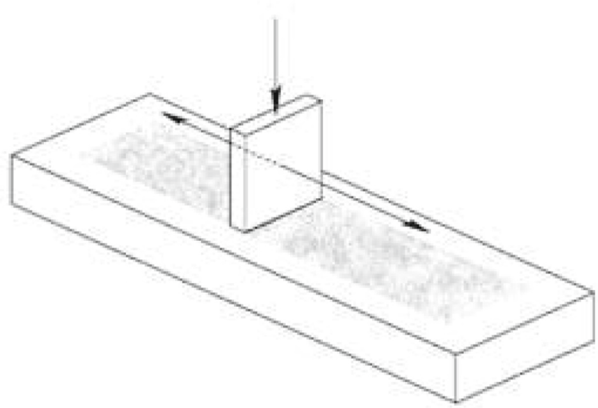

(b) Schematic illustration of the contacting specimens, the moving top specimen has dimensions of 10 x 10 x 2 mm, whilst the stationary bottom specimen has dimensions of 58 x 18 x 5 mm.

Fig. 3. The experimental set-up: schematic, geometry and typical result.

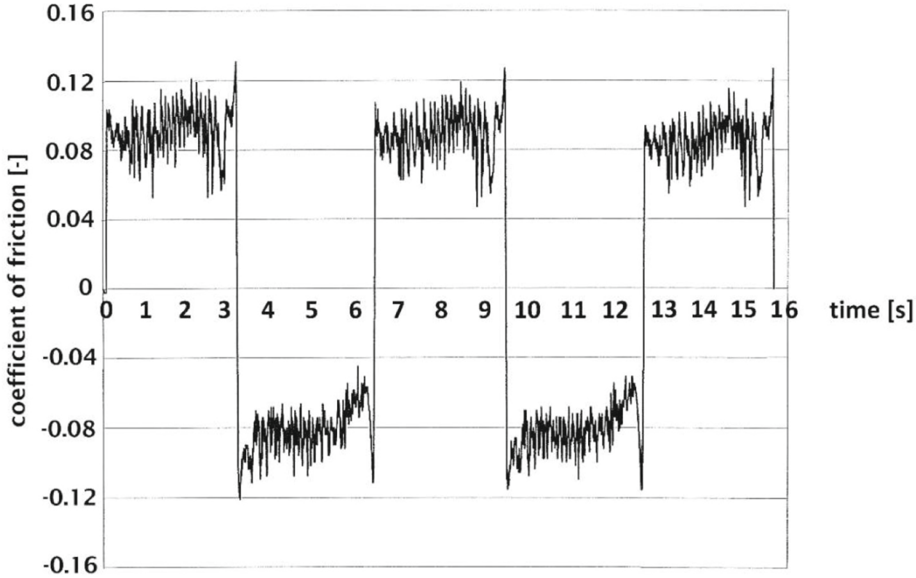

(c) Typical measurement result: coefficient of friction measured between milky quartz and oak, end face

Fig. 3. (*continued*).

Table 2
Experimental conditions in the reciprocating sliding test.

Contact Situation	Flat on flat, Reciprocating Motion
Lubrication	None (dry sliding)
Maximum Sliding Velocity	24 mm·s^{-1}
Motion Amplitude	24 mm
Top Sample (Moving) Material	Flint, Quartzite, Milky Quartz, Lydite
Size	10 × 10 × 2 mm
Bottom Sample (Stationary) Material	Pine Wood, Oak, Bovine Bone
Orientation	Woods: Along grain, Across Grain, End face Bone: Along cells, End face, 'Unspecified': R1, R2, R3
Size	58 × 18 × 5 mm
Apparent Contact Area	20 mm^2
Average Contact Pressure	~ 1 MPa
Test duration	100 cycles 10.5 min
Material combinations tested	Pine v all minerals Oak v all minerals Bone v lyddite only

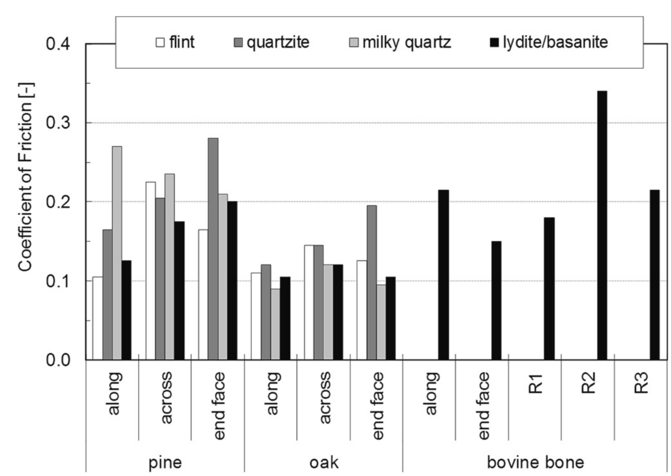

Fig. 4. Measured coefficients of friction for four types of mineral stones sliding against various pine, oak and bovine bone samples.

3.2. Friction Results

Fig. 4 shows the thus obtained coefficients of friction for the four minerals against the various types and orientations of woods and bovine bone.

These results can be summarised as:

- Typical variations in the measured coefficient of friction were approximately 0.02, as shown in Fig. 3(c).
- For pine wood, the measured values for the coefficients of friction show considerable differences between the four stone types and range from 0.1 for flint sliding along the pine grain to almost 0.3 for quartzite against the end face.
- For oak, particularly along and across the grain of the wood, the values are more constant, ranging between 0.09 and 0.15, and no clear differences are found between the various stones.
- For both oak and pine wood the highest value of the coefficient of friction is obtained in the contact between quartzite against the end face of the wood: $\mu = 0.28$ for pine wood and $\mu = 0.19$ for oak.
- For bone, the coefficients of friction measured against lydite are somewhat higher than those measured for both woods against lydite, and range between 0.15 and 0.34. A large influence of the cell-orientation of the bone was found.

The stone specimens were visually inspected after testing. No obvious signs of a glossy patch, indicative of a transition to high-quartz, was observed.

4. Temperature Calculations

Using the highest respective coefficients of friction for pine ($\mu_{max} =$

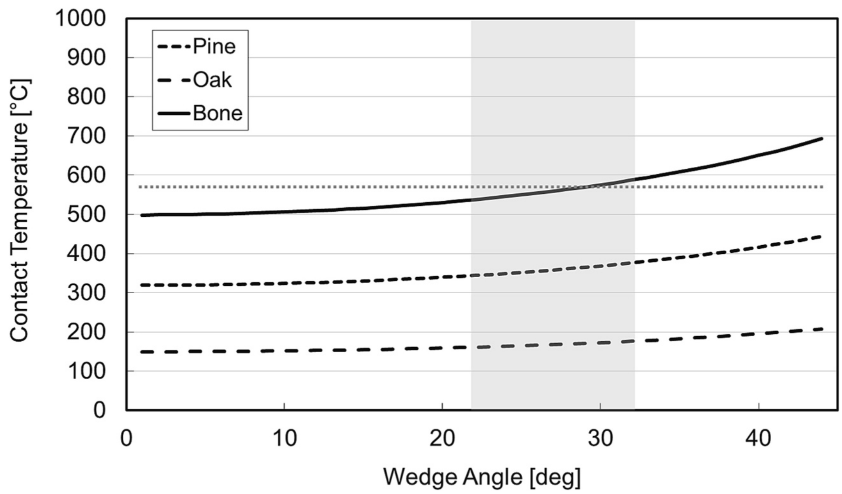

Fig. 5. Calculated Contact Temperatures as a function of the geometry of the stone tool for three different counter surfaces: pine, oak and bone.

0.28), oak ($\mu_{max} = 0.19$) and bone ($\mu_{max} = 0.34$) measured against the various stones, the contact temperatures can be calculated using Eq. (3). In Fig. 5, the resulting temperatures are illustrated as a function of the wedge angle of the stone. The grey area represents the typical wedge angles on the stone tools. The graph shows clearly that for pine wood and oak the critical temperature of 574 °C for the phase transformation to high quartz is not reached. However, for bone against lydite the contact temperature ranges between 550 °C and 600 °C depending on the wedge angle of the tool.

5. Final Remarks

The hypothesis in this work was that friction-induced elevated temperatures that occur in the contact between stone tools and '*work pieces*' of bone and wood cause a phase transformation to high quartz and, hence, the glossy patches that are observed on the stones. These patches are not observed on the stone-stone contact on the working point of the tool, apparently ruling out stone-stone contact during impact or manufacture of the stone tools. Using friction measurements on a range of wood, stone and bone samples and estimating the usage conditions of the stone tools, the flash temperatures in the contact were calculated. The results indicate that sufficiently high temperatures due to frictional heating are observed in the interaction between bone and stone tools, indicating that the glossy patches may be the result of cleaving bone. For the tested wood samples the measured coefficients of friction were too low for any phase transformations to occur. It needs to be noted that the applied test is a simplification of the actual cleaving process. An improved test would include impact to ensure the energy input into the tribo-contact is more representative. Furthermore, fresh wood and bone will have different properties than the used carefully prepared specimens, e.g. in terms of toughness and moisture content. Finally, the observed coefficients of friction, particularly for oak against the stone samples ($\mu \sim 0.1$), are rather low for dry sliding conditions warranting a further investigation into their potential use in mildly loaded engineering applications.

Declaration of Competing Interest

The authors declare that they have no known competing financial interests or personal relationships that could have appeared to influence the work reported in this paper.

Data availability

The data that has been used is confidential.

References

[1] A. Gluchy, R. Vargiolu, C. Mordant, H. Zahouani, Tribology's contribution to archaeology, Surf. Eng. 24 (2) (2008) 154–161.
[2] G.M. Erickson, M.A. Sidebottom, D.I. Kay, K.T. Turner, N. Ip, M.A. Norell, W. G. Sawyer, B.A. Krick, Wear biomechanics in the slicing dentition of the giant horned dinosaur triceratops, Sci. Adv. 1 (5) (2015), e1500055.
[3] G.C.L. Vlamings, Gebruikssporen op stenen uit de Gooise stuwwal, Westerheem AWN 42 (1) (1993) 18–25.
[4] G.H.J. Ruegg, De kwartaire geologie van het Gooi, Mededelingen Mus. Gooi Omstreken VIII (1963) 61–82.
[5] G.H.J. Ruegg, De geologische ontwikkeling van het Gooi gedurende het Kwartair, Geogr. Tijdschrift IX (3) (1975) 202–213.
[6] C.S. Hurlbut, Dana's manual of mineralogy, 18th ed., 1971. ISBN 0471422258.
[7] H. Blok, Theoretical study of temperature rise at surfaces of actual contact under oiliness lubricating conditions, in: Proceedings of the General Discussion on Lubrication and Lubricants vol. 2, Inst. Mech. Engrs, London, 1937, pp. 222–235.
[8] J.C. Jaeger, Moving sources of heat and the temperature at sliding contacts, Proc. Roy. Soc. 76 (1943) 203–224.
[9] J.F. Archard, The temperature of rubbing surfaces, Wear 2 (1958) 438–455.
[10] J. Bos, Frictional heating of tribological contacts, PhD thesis, University of Twente, 1995. ISBN 9090089209.
[11] R. Bosman, M.B. de Rooij, Transient thermal effects and heat partition in sliding contacts, J. Tribol. 132 (2) (2010).
[12] H. Moes, Lubrication and beyond, University of Twente, 2000 accessible at, http://www.utwente.nl/ctw/tr/Research/Publications/Books/book2000b/.
[13] R.C. Weast, Handbook of chemistry and physics, 1st student edition, CRC Press, 1988. ISBN 0849307406.
[14] The engineering toolbox. http://www.engineeringtoolbox.com, 2023.
[15] D. Planck, Eiszeit, kunst und kultur, J.Thorbecke Verlag, Ostfildern, 2009. ISBN 3799508333.
[16] R. Lewin, The origin of modern humans, The Scientific American Library, New York, 1995. ISBN 0716760231.